# Application of benthic foraminiferal Mg/Ca ratios to questions of Cenozoic climate change

K. Billups [a,*], D.P. Schrag [b]

[a] College of Marine Sciences, University of Delaware, 700 Pilottown Road, Lewes, DE 19958, USA
[b] Laboratory for Geochemical Oceanography, Department of Earth and Planetary Sciences, Harvard University, 20 Oxford Street, Cambridge, MA 02138, USA

## Abstract

We investigate the evolution of Cenozoic climate and ice volume as evidenced by the oxygen isotopic composition of seawater ($\delta^{18}O_{sw}$) derived from benthic foraminiferal Mg/Ca ratios to constrain the temperature effect contained in foraminiferal $\delta^{18}O$ values. We have constructed two benthic foraminiferal Mg/Ca records from intermediate water depth sites (Ocean Drilling Program sites 757 and 689 from the subtropical Indian Ocean and the Weddell Sea, respectively). Together with the previously published composite record of Lear et al. [Science 287 (2002) 269–272] and the Neogene record from the Southern Ocean of Billups and Schrag [Paleoceanography 17 (2002) 10.1029/ 2000PA000567], we obtain three, almost complete representations of the $\delta^{18}O_{sw}$ for the past 52 Myr. We discuss the sensitivity of early Cenozoic Mg/Ca-derived paleotemperatures (and hence the $\delta^{18}O_{sw}$) to assumptions about seawater Mg/Ca ratios. We find that during the middle Eocene ($\sim 49$–40 Ma), modern seawater ratios yield Mg/Ca-derived temperatures that are in good agreement with the oxygen isotope paleothermometer assuming ice-free conditions. Intermediate waters cooled during the middle Eocene reaching minimum temperatures by 40 Ma. The corresponding $\delta^{18}O_{sw}$ reconstructions support ice growth on Antarctica beginning by at least 40 Ma. At the Eocene/Oligocene boundary, Mg/Ca ratios (and hence temperatures) from Weddell Sea site 689 display a well-defined maximum. We caution against a paleoclimatic significance of this result and put forth that the partitioning coefficient of Mg in benthic foraminifera may be sensitive to factors other than temperature. Throughout the remainder of the Cenozoic, the temporal variability among $\delta^{18}O_{sw}$ records is similar and similar to longer-term trends in the benthic foraminiferal $\delta^{18}O$ record. An exception occurs during the Pliocene when $\delta^{18}O_{sw}$ minima in two of the three records suggest reductions in global ice volume that are not apparent in foraminiferal $\delta^{18}O$ records, which provides a new perspective to the ongoing debate about the stability of the Antarctic ice sheet. Maximum $\delta^{18}O_{sw}$ values recorded during the Pleistocene at Southern Ocean site 747 agree well with values derived from the geochemistry of pore waters [Schrag et al., Science 272 (1996) 1930–1932] further highlighting the value of the new Mg/Ca calibrations of Martin et al. [Earth Planet. Sci. Lett. 198 (2002) 193–209] and Lear et al. [Geochim. Cosmochim. Acta 66 (2002) 3375–3387] applied in this study. We conclude that the application of foraminiferal Mg/Ca ratios allows a refined view of Cenozoic ice volume history despite uncertainties related to the geochemical cycling of Mg and Ca on long time scales.
© 2003 Elsevier Science B.V. All rights reserved.

* Correspondence author. Tel.: +1-302-645-4249; Fax: +1-302-645-4007.
E-mail addresses: kbillups@udel.edu (K. Billups), schrag@eps.harvard.edu (D.P. Schrag).

## 1. Introduction

Benthic foraminiferal oxygen isotope ratios provide a detailed and continuous perspective on the glacial evolution of the Antarctic ice sheet since the early Cenozoic. Because polar ice sheets sequester the lighter oxygen isotope, their growth and decay brings about changes the $^{18}O/^{16}O$ ratio in seawater, which are preserved in the oxygen isotopic composition of foraminifera. Since the 1970s a number of studies have sought to assess Antarctic glacial evolution on the basis of foraminiferal $\delta^{18}O$ records. Although only coarse temporal resolution at first, these early studies revealed that Antarctica had been glaciated for most of the Cenozoic [1,2]. A more recent compilation of foraminiferal $\delta^{18}O$ records supports the hypothesis that the onset of Antarctic glaciation occurred during the late Eocene [3]. Because of the improved temporal resolution, the new records provide a detailed view of changes in Antarctic glaciation from tectonic to orbital time scales [3].

Benthic foraminiferal $\delta^{18}O$ records have provided significant insights into the history of Antarctic glaciation, but the absolute magnitude of ice extent is difficult to constrain with this method alone. Regional differences in the oxygen isotopic composition of seawater ($\delta^{18}O_{sw}$) may contribute to the global ice volume signal recorded in a foraminiferal test. Over long time scales, the isotopic composition of seawater may not be linearly related to the amount of ice at the poles, but should also vary as function of the isotopic composition of the ice [2]. More importantly, temperature dependent oxygen isotope fractionation during calcification limits the use of foraminiferal $\delta^{18}O$ values as a quantitative proxy for ice volume fluctuations.

Benthic foraminiferal Mg/Ca ratios have become an increasingly popular proxy to reconstruct paleotemperatures. In conjunction with foraminiferal $\delta^{18}O$ values this independent temperature constrain can be used to assess changes in the $\delta^{18}O_{sw}$ through time. Studies focusing on the

Pleistocene avoid uncertainties related to temporal changes in Mg/Ca ratios of seawater on longer time scales [4,5]. Lear et al. [6] were the first to present a benthic foraminiferal Mg/Ca record that spans the entire Cenozoic. Although at low temporal resolution and based on multiple species of benthic foraminifera from different core locations, they were able to address large scale changes in the timing of Cenozoic global ice volume changes. More recently Billups and Schrag [7] demonstrated that benthic foraminiferal Mg/Ca ratios can be used to constrain changes in the $\delta^{18}O_{sw}$ during the Neogene and yield a refined estimate of individual middle to late Miocene sea level changes.

In this paper we revisit the Cenozoic evolution of Antarctic glaciation. We present results from two benthic foraminiferal Mg/Ca records. Ocean Drilling Program (ODP) site 757, for which we have a complete record that spans the past 52 Myr, is presently located at intermediate water depths in the subtropical Indian Ocean (Fig. 1, Table 1). ODP site 689 lies at intermediate water depth in the Weddell Sea and spans the early Eocene to late Oligocene climate transition (Fig. 1, Table 1). Together with the previously published composite record of Lear et al. [6] and the intermediate water depth Neogene record from the Southern Ocean of Billups and Schrag [7], we obtain three, almost complete representations of the $\delta^{18}O_{sw}$ for the past 52 Myr. On these long timescales, $Mg^{+2}$ and $Ca^{+2}$ concentrations in seawater may not have remained constant, and we discuss the sensitivity of early Cenozoic Mg/Ca-derived paleotemperatures (and hence the $\delta^{18}O_{sw}$) to assumptions about seawater Mg/Ca ratios.

## 2. Methods

### 2.1. Site selection

We chose ODP sites 757 and 689 because they are located at intermediate water depths and have low sedimentation rates. We focus on intermedi-
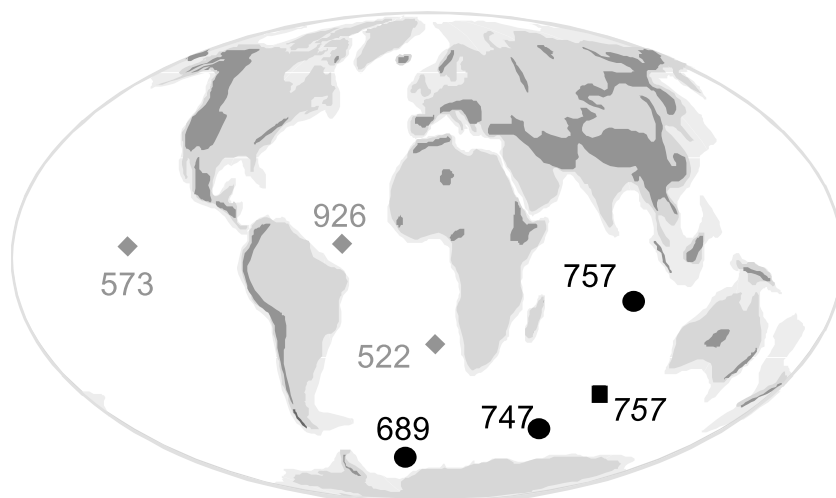
Fig. 1. Locations of sites investigated in this study. Details are given in Table 1. The square marks the position of site 757 during the early Eocene. Gray diamonds indicate the locations of the sites used by Lear et al. [6] to construct the composite record (which also includes a short portion of site 689).

ate water depths sites to assure that the sediments remained above the inferred level of the calcium carbonate compensation depth during the Paleocene and Eocene [8] minimizing the potential effects of carbonate dissolution and/or changes in carbonate ion concentration relative to saturation on benthic foraminiferal Mg/Ca ratios [9,10]. Low sedimentation rates offer the advantage that diagenetic effects associated with high overburden pressure and temperature may be minimized [11].

Site 757, on the Ninetyeast Ridge, was located in the Southern Ocean (45°S) during the early

Eocene ($\sim$50 Ma) and since then has drifted north to its present day subtropical position at 17°S [12] (Fig. 1; Table 1). In the modern ocean, the meridional temperature gradient between 45°S and 17°S at 1650 m water depth is less than 1°C [13], and we assume that a geographic temperature effect on benthic foraminiferal Mg/Ca ratios was likewise small over the course of the Cenozoic. The Ninetyeast Ridge was subaerially exposed during the late Paleocene, but site 757 had moved to within 100 m of its present depth of 1650 m by the early Eocene [12]. Thus we can also rule out

Table 1
Location of ODP and Deep Sea Drilling Project (DSDP) sites discussed in this study

| Site | Long. (°) | Lat. (°) | Paleolat.[a] (°) | Depth (m) | Paleodepth[b] (m) | Time interval (Ma) |
|------|-----------|----------|------------------|-----------|-------------------|--------------------|
| ODP 757 | 88°E | 17°S | 45°S | 1652 | 1500 | 0–52 |
| ODP 689 | 03°E | 65°S | N/A | 2080 | 1400–1650 | 30–44 |
| ODP 689[c] | 03°E | 65°S | N/A | 2080 | 1400–1650 | 37–48 |
| ODP 747[d] | 77°E | 55°S | N/A | 1695 | N/A | 0–26 |
| DSDP 522 | 26°S | 05°W | N/A | 4400 | 3000 | 32–35 |
| DSDP 573 | 0°N | 134°W | N/A | 4300 | 4300–3000 | 0–35 |
| ODP 926 | 4°N | 43°W | N/A | 3600 | 3500 | 6–12 |

[a] Paleolatitude of site 757 refers to the latitude during the early Eocene (50 Ma) [12].
[b] Site 689: water depth during the early Cenozoic (50–35 Ma) [14]; site 757: water depth during the early Eocene (50 Ma) [12].
[c] Site 689 portion of the Lear et al. [6] composite record.
[d] Billups and Schrag [7].

that the vertical thermal gradient dominated foraminiferal Mg/Ca ratios. Sedimentation rates average $\sim 1$ m/Myr, but decrease by almost an order of magnitude during the latest Oligocene through early Miocene [12].

Site 689 is located on Maud Rise in the Weddell Sea (Fig. 1; Table 1). The core location subsided by $\sim 250$ m during the middle Eocene [14], but we assume that the effect of a temperature change associated with sinking of the core location from 1400 m to 1650 m was small. Sedimentation is continuous at rates averaging $\sim 6$ m/Myr [14].

## 2.2. Age control

Age models at all sites reflect the Berggren et al. [15] time scale. At site 757 a published $\delta^{18}O$ record that spans the earliest Cenozoic (36–52 Ma) has been updated to Berggren et al. [15] by Zachos et al. [3]. We added $\delta^{18}O$ measurements between 30 Ma and 40 Ma to capture the Eocene/Oligocene boundary, and we use the associated rapid $\delta^{18}O$ shift at 33.65 Ma to adjust the age model for this 10 Myr long time slice to the Berggren et al. [15] time scale (the age–depth con-

trol point is included in Table 2). For the youngest portion of the record (0–30 Ma) we use the Leg 121 shipboard calcareous nannofossil biostratigraphy updating the ages of datums to those given by Berggren et al. [15,16] (Table 2). At site 689 we sampled intervals adjacent to the $\delta^{18}O$ record of [14]. The age model of this site was updated to [15] by Zachos et al. [3]. The age model for site 747 was updated to [15] by Billups and Schrag [7]. The age model of the composite record of [6] is also consistent with [15], at least during critical intervals such as the Eocene/Oligocene boundary.

## 2.3. Analytical methods

Bulk sediment and sample processing followed standard procedures described in detail by Billups and Schrag [7]. Between 5 and 15 benthic foraminifera of the genus *Cibicidoides* (site 757: *Cibicidoides wuellerstorfi* between $\sim 0$ and 14 Ma; *Cibicidoides mundulus* between $\sim 0$ and 20 Ma; *Cibicidoides* spp. between 20 and 52 Ma; site 689: *Cibicidoides* spp.) were picked from the 250–425 μm size fraction, crushed between two glass plates and prepared for minor elemental analyses. The crushed samples were repeatedly sonicated in deionized water and methanol to remove adhering sediment, sonicated in 1 M NH$_4$Cl to remove exchangeable ions, and boiled in alkaline peroxide solution (0.15% H$_2$O$_2$ in 0.1 N NaOH) for 10 min (sonicating once) to oxidize organic contaminants. Our methodology follows the procedures of Brown and Elderfield [9], Hastings et al. [17], and Lear et al. [6], which does not include a reductive cleaning step. More recent investigations into cleaning methods, however, suggest that the addition of the reducing step can lower Mg/Ca ratios in some samples (e.g., by 0.13 mmol/mol) but it is not yet clear whether this effect is species-specific or site-specific [18]. Other effects such as high Mg calcite contamination, rather than cleaning vigor, may pose an additional source of data scatter (e.g., on the Little Bahama Banks, [19]). Because we are investigating long-term trends that are defined by relatively large changes in benthic foraminiferal Mg/Ca ratios apparent at more than one site, we do not

Table 2
Summary of age–depth control points for the Pleistocene through Oligocene at site 757

| Datum | Depth (mbsf)[a] | Age (Ma)[b] |
|---|---|---|
| LO *Pseudoemiliania lacunosa* | 3.05 | 0.46 |
| LO *Calcidiscus macintyrei* | 9.75 | 1.59 |
| LO *Discoaster brouweri* | 12.75 | 1.95 |
| LO *Discoaster tamalis* | 16.30 | 2.78 |
| LO *Reticulofenestra pseudoumbilica* | 23.30 | 3.75 |
| FO *Ceratolithus acutus* | 38.95 | 5.34 |
| LO *Discoaster quinqueramus* | 43.55 | 5.6 |
| FO *Amaurolithus primus* | 53.25 | 7.2 |
| LO *Discoaster hamatus* | 71.50 | 9.4 |
| LO *Sphenolithus heteromorphus* | 83.75 | 13.6 |
| FO *Sphenolithus heteromorphus* | 96.10 | 18.2 |
| FO *Sphenolithus belemnos* | 99.45 | 19.2 |
| FO *Discoaster druggii* | 100.5 | 29.9 |
| FO *Sphenolithus ciperoensis* | 106.5 | 29.9 |
| Eocene/Oligocene boundary | 120.3–121.8 | 33.65 |

[a] Depth in the core as meters below sea floor (mbsf) is the midpoint of the depth range given in [12].
[b] Ages for the Oligocene through Miocene (29.9–5.6 Ma) are from [15]; Plio/Pleistocene (5.3–0.46 Ma) from [16].

believe that the omission of the reducing step has significantly affected our data interpretations. Each cleaning step was followed by one rinse plus three sonication steps in DI water to ensure complete removal of the waste solution. Depending on the amount of material, cleaned samples were dissolved in 0.4–0.7 ml of 2% trace metal clean $HNO_3$ to obtain a solution of between 10 and 120 ppm Ca. Mg/Ca ratios were measured on an Inductively Coupled Plasma Atomic Emissions Spectrophotometer at Harvard University. Matrix effects were constrained by analyzing five to six standard solutions of differing $Ca^{2+}$ concentration and Mg/Ca ratios, a method outlined in detail by Schrag [20]. Analytical precision based on analyses of a reference standard solution is better than 0.3%. At site 757 we were able to obtain a number of sample splits of *C. wuellerstorfi* and *C. mundulus*; with only few exceptions the replicate analyses lie within ∼5% (Appendix 1 **Background Data Set**[1]). As detailed by Billups and Schrag [7] at this site we were also able to obtain *C. wuellerstorfi* and *C. mundulus* measurements from the same sample intervals (Appendix 1 **Background Data Set**[1]), and we correct *C. wuellerstorfi* Mg/Ca ratios to *C. mundulus* by adding 0.2 mmol/mol. We were not able to determine a species offset between *C. mundulus* and *Cibicidoides* spp., which are prevalent in the pre Miocene intervals. All Mg/Ca data (as average ratios from each interval) are given in Appendix 2 **Background Data Set**[1].

For age model purposes, we carried out 23 oxygen isotope analyses (not shown but added to Appendix 2 **Background Data Set**[1]) on three to five tests of *Cibicidoides* spp. at site 757. Stable isotope ratios were measured following standard procedures using the VG Optima dual inlet isotope ratio mass spectrometer equipped with a common acid bath located at Harvard University. Prior to analysis samples were ultrasonically cleaned, crushed to ensure speedy reaction, and oven dried. Based on replicate analysis of in-house standards the precision is better than 0.08‰.

---

[1] http://www.elsevier.com/locate/epsl

## 2.4. Calculation of paleotemperatures and the $\delta^{18}O$ of seawater

Martin et al. [10] and Lear et al. [19] provide new Mg/Ca to temperature calibrations that incorporate different *Cibicidoides* species (e.g., *C. wuellerstorfi*, *C. pachyderma*, *C. compressus*) and a wider range of temperatures than the previous calibration of Rosenthal et al. [21]. We use the equation of Lear et al. [19], which contains the Martin et al. [10] data set. For the purpose of comparing our new Cenozoic $\delta^{18}O_{sw}$ records to published ones, we also apply the new regression to the Neogene Mg/Ca record from Southern Ocean site 747 [7] and the composite Mg/Ca record of Lear et al. [6]. To calculate $\delta^{18}O_{sw}$ we assume modern oceanic Mg/Ca ratios. This assumption may be oversimplified, and we estimate the effect of varying seawater Mg/Ca ratios on absolute temperature reconstructions of the middle Eocene.

To calculate the $\delta^{18}O_{sw}$ from the Mg/Ca-based temperatures, we use the composite benthic foraminiferal $\delta^{18}O$ record of Zachos et al. [3] (Fig. 2, top panel). The Eocene portion of the composite record incorporates measurements from sites 689 and 757, and thus corresponds directly to our Mg/Ca records. At site 747 we have paired Mg/Ca and $\delta^{18}O$ values [7] and we use them. We solve the paleotemperature equation of Shackleton [22] for the $\delta^{18}O_{sw}$ using Mg/Ca-derived temperatures together with the foraminiferal $\delta^{18}O$ values. This equation has the advantage that it is calibrated using benthic foraminifera of the genus *Uvigerina*, and *Cibicidoides* to *Uvigerina* $\delta^{18}O$ offsets have been constrained (+0.64‰, e.g., [23]).

## 3. Results

There is a relatively large amount of data scatter during the Eocene and Oligocene portions of the sites 757 and 689 Mg/Ca records, and high ratios of up to 6.6 mmol/mol are apparent during the early Eocene (site 757) (Fig. 2, middle panel). Sources of the variability include interspecies differences in Mg/Ca ratios, insufficient cleaning, and calcite recrystallization. Interspecies offsets
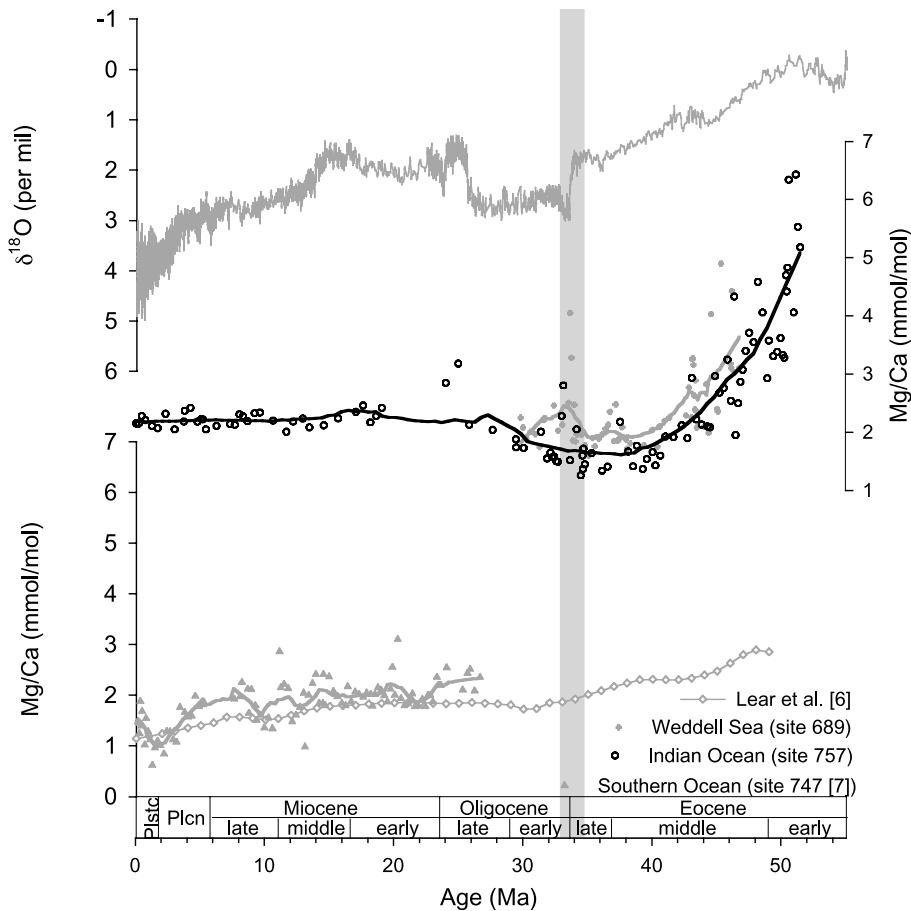
Fig. 2. Comparison of the Cenozoic benthic foraminiferal composite $\delta^{18}O$ record [3] (top panel) to benthic foraminiferal Mg/Ca records from Indian Ocean site 757 and Weddell Sea site 689 (middle panel). The solid lines reflect a 20% exponential smoothing function through the site 757 (black) and site 689 (gray) data. The bottom panel shows the published composite Mg/Ca record of Lear et al. [6], which has been smoothed to a 1 Myr temporal resolution, and the Southern Ocean record from site 747 of Billups and Schrag [7]. The gray line reflects a 10% exponential smoothing function through the site 747 data. The vertical gray band highlights the Eocene/Oligocene boundary (33.65 Ma, Berggren et al. [15]).

can be as large as 1 mmol/mol [6], and it is possible that offsets exist among *Cibicidoides* spp. used in this study. Insufficient cleaning (omission of the reductive step) may present a problem if metal oxides, which are removed during this procedure [24], are primarily present in the most deeply buried samples. Another potential source of data scatter may be calcite recrystallization in the deepest portion of the sedimentary column. The partitioning coefficient of Mg for abiotic calcite is two orders of magnitudes higher than that of biogenic calcite [25], and the addition of diage-

netic calcite would increase foraminiferal Mg/Ca ratios. To avoid interpretation of singular data points, we have smoothed the Mg/Ca data at both sites (Fig. 2, middle panel). It is the parallel trend of decreasing ratios during the middle Eocene that leads us to believe that interspecies offsets, cleaning protocol, and diagenetic effects are relatively minor.

The smoothed Mg/Ca records agree with the earlier study of Lear et al. [6] in that there is an overall decrease in benthic foraminiferal Mg/Ca ratios over the course of the Cenozoic, but on

the finer scale some important differences exist (Fig. 2). Most notably, Mg/Ca ratios at sites 757 and 689 display a much larger range during the early Cenozoic. Benthic foraminiferal Mg/Ca ratios at Indian Ocean site 757 and Weddell Sea site 689 are both highest during the early to middle Eocene and decrease rapidly until ∼40 Ma (Fig. 2, middle panel). In contrast, the composite Mg/Ca record of Lear et al. [6], which has been smoothed to a resolution of 1 Myr, lacks a pronounced Eocene maximum and ratios decrease more gradually until the early Oligocene (Fig. 2, bottom panel). At site 757, ratios begin to increase gently after 40 Ma and remain relatively constant after the late Oligocene (Fig. 2, middle panel). At site 689, Mg/Ca ratios show considerable variability after ∼40 Ma as defined by a small maximum at the middle to late Eocene transition and a well-defined maximum coincident with the Eocene/Oligocene boundary (Fig. 2, middle panel). During the Neogene there is a tendency toward lower ratios in the composite record of Lear et al. [6] and the Southern Ocean record from site 747 (Fig. 2, bottom panel).

Paleotemperature reconstructions from sites 757 and 689, which assume modern seawater ratios throughout the Cenozoic, illustrate that early Cenozoic cooling of intermediate waters occurred prior to the first major episode of Antarctic ice growth at the Eocene/Oligocene boundary (Fig. 3, middle panel). Sites 757 and 689 display a temperature minimum at ∼40 Ma. At site 689, temperatures increase by ∼2°C toward the Eocene/Oligocene boundary and decrease again thereafter. Site 757 displays a gradual temperature increase between the late Eocene and late Oligocene, but the temperature remains constant through the Neogene. This lack of temperature variability is odd and results in unrealistically high temperature estimates for the Pleistocene (∼8°C). For comparison, the composite deep water record of Lear et al. [6] shows a temperature minimum at ∼30 Ma, relatively constant temperatures during the Oligocene, and a gradual cooling trend during the early Miocene. Both the Lear et al. [6] and the Southern Ocean record from site 747 display cooling trends beginning in the late Miocene, and

Pleistocene temperatures between 1 and 4°C agree better with modern ocean conditions.

To minimize the effect of transient Mg/Ca excursions on the $\delta^{18}O_{sw}$ reconstructions (e.g., the Mg/Ca and temperature maximum at the Eocene/Oligocene boundary at site 689), we average the (smoothed) temperature records to 1 Myr intervals. The Lear et al. [6] record has already been smoothed to 1 Myr intervals. As discussed by Lear et al. [6], there is an overall increase in the calculated $\delta^{18}O_{sw}$ over the past 50 Myr, which agrees well with the increases in foraminiferal $\delta^{18}O$ values and the Cenozoic trend toward polar glaciation (Fig. 3, bottom panel). There is a general agreement among the records in the timing of $\delta^{18}O_{sw}$ maxima and minima. All records display a $\delta^{18}O_{sw}$ minimum during the middle Eocene, although the exact timing differs between sites 757 and 689 (both at 40 Ma) and the composite record of Lear et al. [6] (at 49 Ma). The $\delta^{18}O_{sw}$ record from sites 757 and 689 both imply that ice growth began at 40 Ma; the Lear et al. [6] record would accommodate an earlier onset of Antarctic glaciation. The absolute magnitude of the $\delta^{18}O_{sw}$ minimum in each instance (−1.3‰, Lear et al. [6] composite record; −0.9‰, site 689; −1.3‰, site 757) agrees well with $\delta^{18}O_{sw}$ values derived from oxygen isotope mass balance assuming an ice-free world (e.g., −0.9 to −1.2‰ depending on assumptions of the isotopic composition of the ice sheet, −25‰ and −35‰, respectively). After the middle Eocene minimum, the $\delta^{18}O_{sw}$ at sites 689 and 757 increases gradually at first by 0.4‰ and then all records show an additional rapid increase of 1‰ across the Eocene/Oligocene boundary. At Indian Ocean site 757 and in the Lear et al. [6] composite record the $\delta^{18}O_{sw}$ decreases rapidly during the late Oligocene (∼26 Ma) at about the same time as benthic foraminiferal $\delta^{18}O$ values (Fig. 3, bottom and top panels, respectively). Excellent agreement among records also exists during the early Miocene when all $\delta^{18}O_{sw}$ records decrease toward a minimum at ∼16 Ma, the early Miocene climatic optimum, followed by an increase in $\delta^{18}O_{sw}$, the second major phase of Antarctic ice growth [1], after which all records continue to increase through the late Miocene. During the Pliocene, the Lear et al. [6] composite
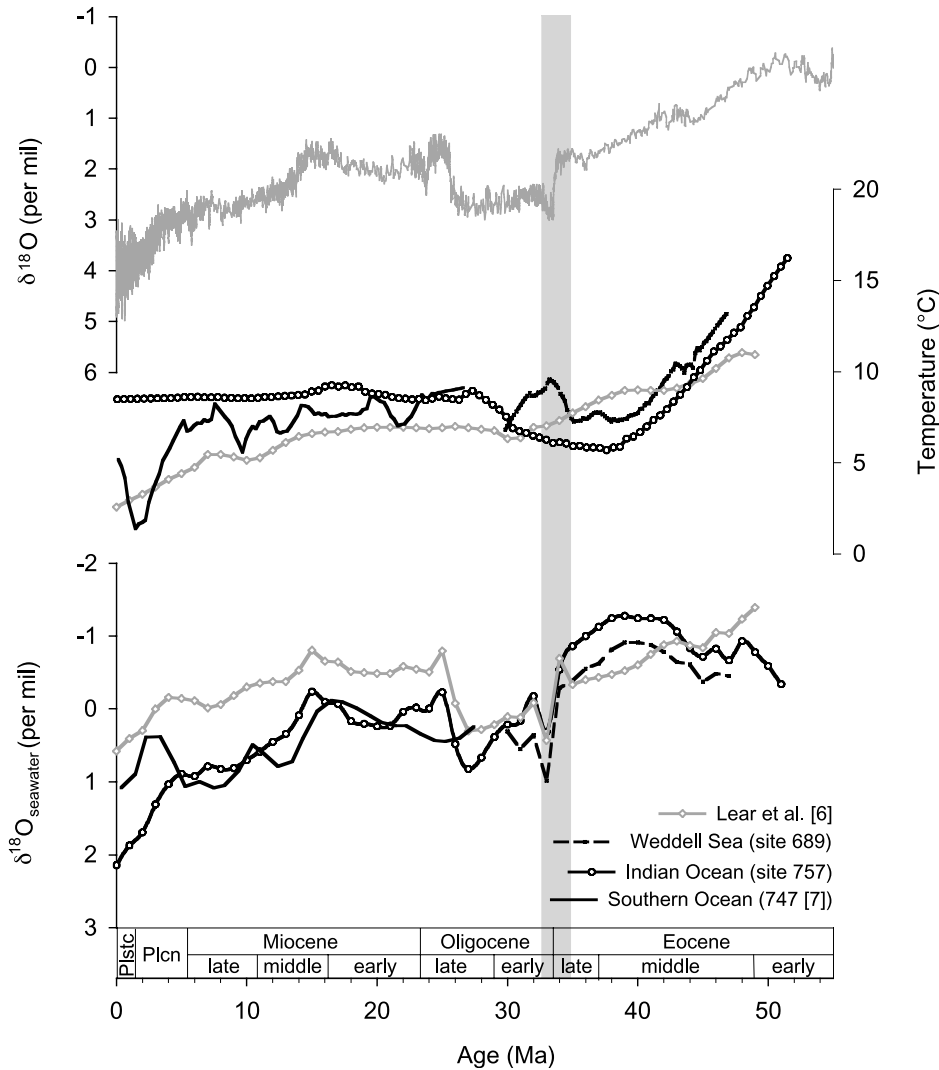
Fig. 3. Comparison of the Cenozoic benthic foraminiferal composite $\delta^{18}O$ record [3] (top panel) to temperature records derived from the smoothed benthic foraminiferal Mg/Ca records (middle panel) and $\delta^{18}O_{sw}$ records (bottom panel). Each of the $\delta^{18}O_{sw}$ records has been averaged to 1 Myr intervals. The vertical gray band highlights the Eocene/Oligocene boundary (33.65 Ma, Berggren et al. [15]). Temperatures were calculated using the calibration of Lear et al. [19] where Mg/Ca $= 0.867e^{0.109 \times temperature\,(^\circ C)}$. To calculate the $\delta^{18}O_{sw}$ we solve the paleotemperature equation of Shackleton [22]: $\delta^{18}O_{sw} = (temperature\,(^\circ C) - 16.4 + 4*\delta^{18}O_{calcite})/4$.

and the Southern Ocean site 747 $\delta^{18}O_{sw}$ records display minima that do not correspond to minima in the benthic foraminiferal $\delta^{18}O$ record.

The absolute magnitude of $\delta^{18}O_{sw}$ changes differs among the records creating inter-site offsets (Fig. 3, bottom panel). During the Miocene, the $\delta^{18}O_{sw}$ of the two intermediate water records (sites 757 and 747) generally overlap but during

the Plio/Pleistocene site 757 values increase rapidly resulting in unrealistically high $\delta^{18}O_{sw}$ value of $\sim 2\%_o$ during the latest Pleistocene. At site 747, however, a Pleistocene $\delta^{18}O_{sw}$ maximum of $\sim 1\%_o$ agrees well with the $\delta^{18}O_{sw}$ to be expected during full glacial conditions such as during the Last Glacial Maximum [26]. The $\delta^{18}O_{sw}$ record based on the Lear et al. [6] data displays notably
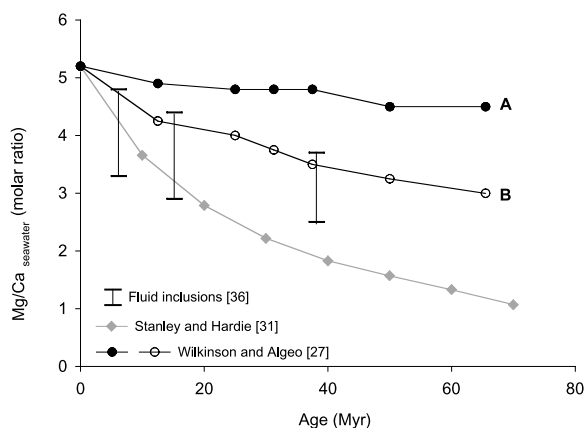
Fig. 4. Cenozoic changes in Mg/Ca ratios of seawater based on three different numerical models plus ratios measured from fluid inclusions in marine halites. The two curves from Wilkinson and Algeo [27] differ in assumptions about residence times of Mg in seawater with respect to hydrothermal circulation. The curve of Stanley and Hardie [31] reflects a two endmember mixing model between river influx and hydrothermal brines taking into account a linear decrease in spreading rates. The Mg/Ca ratios in fluid inclusions display a large range (indicated by the vertical bars) due to uncertainties related to $Ca^{2+}$ concentrations [36].

lower values than those recorded at the intermediate water sites.

## 4. Discussion

### 4.1. Sensitivity of paleotemperatures to seawater Mg/Ca ratios

On long time scales, the application of foraminiferal Mg/Ca ratios to reconstruct absolute paleotemperatures, and hence the $\delta^{18}O_{sw}$, may be limited by the complexity of $Mg^{2+}$ and $Ca^{2+}$ cycling between carbonate and silicate reservoirs. Weathering of limestone, dolomite, and silicate rocks supplies $Mg^{2+}$ and $Ca^{2+}$ to the ocean. Carbonate sedimentation effectively removes $Ca^{2+}$ from seawater. Previous studies have suggested that the importance of dolomite formation decreases during the Cenozoic [27], leaving hydrothermal circulation and associated basalt alteration as the primary sink for Mg and a secondary source of $Ca^{2+}$ [27,28]. Additional minor factors involve the low

temperature alteration of basalt and ion exchange with clays [29,30].

Geochemical models have been used to constrain changes in Mg/Ca ratios through the Phanerozoic [27,31]. During the Cenozoic portion of the model curves (Fig. 4), Mg/Ca ratios tend to increase toward the presence in the two models dominated by a linear decrease in seafloor spreading rates, which serves to decrease the hydrothermal sink of Mg (e.g., in fig. 4 of Stanley and Hardie [31] and the curve labeled B from Wilkinson and Algeo [27]). The second model provided by Wilkinson and Algeo [27] (labeled A in Fig. 4) assumes a constant residence time of 14 Myr for ridge-bound Mg and shows little difference between early Cenozoic and modern seawater ratios. These models do not take into consideration that hydrothermal circulation may change in response to changes in the tectonic regime rather than simply the rate of seafloor spreading [32,33]. Furthermore, the models neglect that the amount of Mg uptake at ridges during hydrothermal circulation may depend on the temperature at the sediment basement interface and the amount of seawater percolating through the crust [34]. In a general sense, fluid inclusions in marine halites [35,36] would support an increase in seawater Mg since the early Cenozoic (Fig. 4), but the range in Mg/Ca ratios is large, reflecting assumptions about $Ca^{2+}$ concentrations [36]. Thus a correction of foraminiferal Mg/Ca ratios for temporal changes in seawater Mg/Ca ratios is difficult to justify. Therefore we use modern ratios, and evaluate the uncertainties associated with this assumption.

Paleotemperatures based on foraminiferal Mg/Ca ratios are sensitive to assumptions of seawater ratios (Fig. 5, Table 3). We illustrate this point using three examples: at 52 Ma ratios are at a maximum, at 48–49 Ma ratios can be compared to the Lear et al. [6] record, and at 40 Ma sites 757 and 689 ratios both reach a minimum. Assuming ice-free conditions, the oxygen isotope paleothermometer provides a check on the Mg-derived temperatures. Accounting for the three different seawater scenarios plus modern ratios results in a Mg-based paleotemperature range of between 28 and 16°C at 52 Ma (Fig. 5a, Table 3). The highest temperature estimate corresponds to

the lowest seawater ratios of Stanley and Hardie [31], and modern seawater ratios yield the lowest temperature. None of these estimates agree with the 12–13°C derived from foraminiferal $\delta^{18}O$ values. Three million years later at 48–49 Ma, we obtain a temperature range of 24–13°C at site 757 and 22–11°C for the Lear et al. [6] composite record (Fig. 5b, Table 3). In both records modern



ratios and the high ratio scenario of Wilkinson and Algeo [27] (curve A in Fig. 4) yield paleotemperatures consistent with the oxygen isotope thermometer (11–13°C) (Fig. 5b, Table 3). Lear et al. [6] Mg/Ca ratios are 0.7 mmol/mol lower than those at site 757, and the agreement with the oxygen isotope thermometer is slightly better. The difference is likely a species offset between *Oridorsalis umbonatus*, the reference species of Lear et al. [6] and *Cibicidoides* spp. used in this study. At 40 Ma modern ratios as well as the high ratio curve from Wilkinson and Algeo [27] yield excellent agreement between the Mg/Ca-derived temperatures (7–9°C) and $\delta^{18}O$-based paleothermometer (7–8°C) (Fig. 5c; Table 3). If the assumption of an ice-free middle Eocene is a good one, then these observations suggest that seawater Mg/Ca ratios were similar to modern ratios, or at most $\sim$0.5 molar ratios lower than today by 48–49 Ma.

The latter two examples highlight the value of the new Mg-temperature calibrations of Martin et al. [10] and Lear et al. [19]. The effect of species offsets (e.g., 0.7 mmol/mol) on the calculated temperature (2°C) appears to be relatively small in this context. Thus, high ratios at site 757 during the early Eocene (52 Ma) may be due to a shallower water depth of the core location, but without $\delta^{18}O$ measurements from these specific intervals we cannot verify this possibility. High
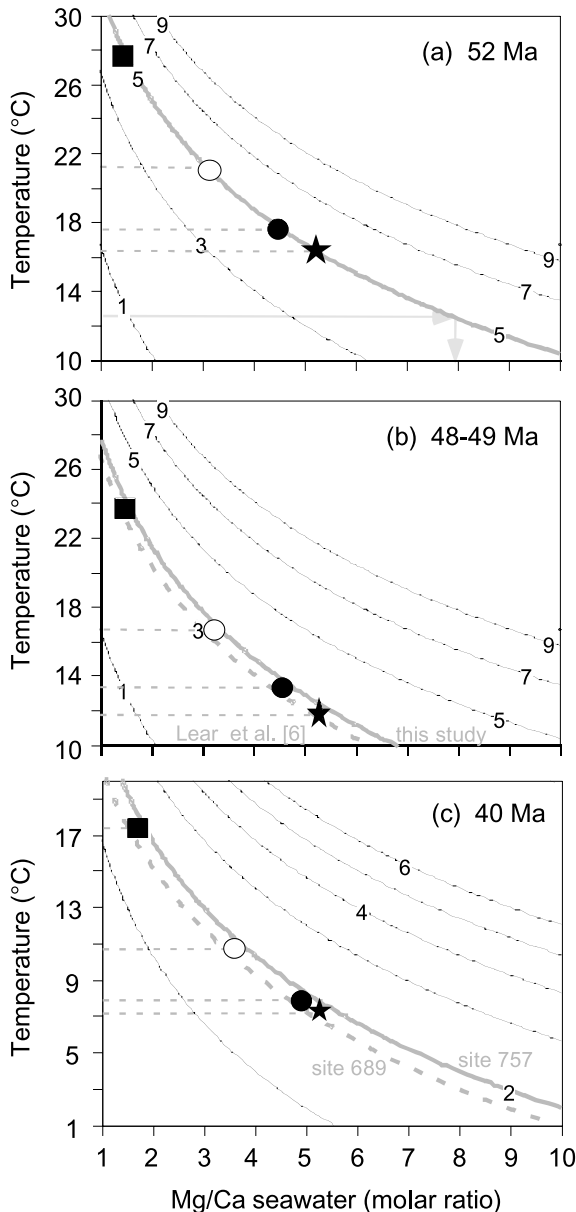
←
Fig. 5. Graphical illustration of the sensitivity of temperature reconstructions (*y*-axis) to seawater Mg/Ca ratios (*x*-axis) at (a) 52 Ma, (b) 48–49 Ma, and (c) 40 Ma. The contours (benthic foraminiferal Mg/Ca ratios in mmol/mol) were derived using the temperature calibration of Lear et al. [19]. The solid square in each panel denotes the intersection between observed foraminiferal Mg/Ca ratios and seawater Mg/Ca ratios of Stanley and Hardie [31], the solid and open circles mark the intersection between observed foraminiferal Mg/Ca ratios and the seawater Mg/Ca curves of Wilkinson and Algeo [27] (A and B in Fig. 4, respectively), and the star indicates the intersection between observed foraminiferal Mg/Ca ratios and modern seawater Mg/Ca ratios [30]. The corresponding temperatures in each scenario can be read off the *y*-axis and are summarized in Table 3. The gray arrows in (a) point to a predicted seawater ratio given averaged foraminiferal Mg/Ca ratios of 5 mmol/mol assuming a $\delta^{18}O$-derived temperature of 12.5°C (see text).

foraminiferal ratios could also reflect high sea-water ratios. At 52 Ma, we would arrive at a predicted seawater Mg/Ca ratio of $\sim 8$ mmol/mol (e.g., Fig. 5a). This estimate clearly disagrees with any of the modeled curves as well as the fluid inclusion data and would imply a rapid decrease in seawater ratios to modern ones between 52 and 48 Ma. Regardless of the cause, $\delta^{18}O_{sw}$ values calculated from Mg/Ca-derived temperatures and the composite $\delta^{18}O$ record between 52 and 49 Ma are questionable. It may be that the largest uncertainty in Mg/Ca-derived temperature reconstructions relates to assumptions about temporal changes in seawater Mg/Ca ratios rather than interspecies offsets, cleaning methods, or diagenesis. Although seawater ratios may have been similar to modern ratios during the middle Eocene, they may not have remained constant since then.

### 4.2. Eocene/Oligocene boundary: temperature versus biogeochemical effects

The Eocene/Oligocene boundary represents one of the most rapid transitions in global climate [3]. Yet, as pointed out by Lear et al. [6], neither the composite nor a high resolution record generated specifically for this purpose show a decrease that would signify deep water cooling concurrent with this event. We observe an increase in intermediate water temperatures at Weddell Sea site 689 during the late Eocene that culminates in a marked temperature maximum coeval with the large foraminiferal $\delta^{18}O$ shift that characterizes the Eocene/Oligocene boundary (Fig. 3, middle panel). Our results could be taken as evidence for the importance of a relatively warm high latitude ocean to fuel an expanding ice sheet with moisture (e.g., the snow gun hypothesis [37]).

However, in light of recent studies that have elucidated the importance of seawater chemistry on elemental ratios in biogenic carbonate [38–40], we put forth that the increase in Mg/Ca ratios at this site could also indicate a sensitivity of the partitioning coefficient of Mg in benthic foraminifera to environmental factors other than temperature. Periods of enhanced primary productivity, as evidenced by site 689 benthic foraminiferal abundance patterns and increases in productivity of siliceous organisms, occurred in the Southern Ocean during the middle Eocene (42–44 Ma), the late Eocene (35 Ma) and most notably at the Eocene/Oligocene boundary (33.5 Ma) [41]. The former two intervals roughly correspond in time to intervals during which we observe relatively high benthic foraminiferal Mg/Ca ratios at site 689 (e.g., Fig. 2). The latter interval, the Eocene/Oli-

Table 3
Sensitivity of Mg-derived paleotemperatures to assumptions of seawater ratios

| Site | Time (Ma) | Mg/Ca calcite (mmol/mol)[a] | $\delta^{18}O$-based temperature (°C)[b] | Mg/Ca seawater (molar ratio)[c] | Mg/Ca-based temperature (°C)[d] |
|------|-----------|------------------------------|------------------------------------------|----------------------------------|----------------------------------|
| 757 | 52 | 5.0 | 12.1–13.3 | 1.5 | 27.5 |
| | | | | 3.2 | 20.5 |
| | | | | 4.5 | 17.4 |
| | | | | 5.2 | 16.1 |
| 757/Lear et al. | 48–49 | 3.6/2.9 | 11.3–12.5 | 1.6 | 23.9/21.9 |
| | | | | 3.3 | 17.2/15.2 |
| | | | | 4.6 | 14.2/12.2 |
| | | | | 5.2 | 13.1/11.1 |
| 757/689 | 40 | 1.8/2.0 | 6.5–7.7 | 1.8 | 16.4/17.4 |
| | | | | 3.5 | 10.3/11.3 |
| | | | | 4.8 | 7.4/8.4 |
| | | | | 5.2 | 7.6/7.7 |

[a] Mg/Ca ratios are averages obtained from the smoothed records (Fig. 2).
[b] The range reflects temperatures using a $\delta^{18}O$ value of the ice of −35 and −25‰.
[c] Seawater ratios in vertical order are from [31], [27] (curves B and A, respectively, in Fig. 4), and the modern ratio.
[d] Temperatures in front of the slash are based on site 757, temperatures after the slash are based on Lear et al. [6] for the 48–49 Ma time interval and from site 689 for the 40 Ma time interval.

gocene boundary coincides with the well-developed maximum in site 689 Mg/Ca ratios (Fig. 2 middle panel). Increased productivity adds to the food supply of benthic organisms and could affect foraminiferal biomineralization rates. However, unlike the partitioning coefficient of Sr, which is positively correlated with calcification rates, or the partitioning coefficients of Co, Mn, and Cd, which are negatively correlated with calcification rates, there is no significant influence of rate on the partitioning coefficient of Mg in inorganic calcite experiments [42–44]. With respect to biogenic calcite, Sr uptake into coccolithophorid calcite is enhanced when environmental conditions support higher growth and calcification rates [39,45]. Culture experiments with planktonic foraminifera illustrate that Sr/Ca ratios tend to increase with seawater pH, which may reflect enhanced calcification in response to a higher carbonate ion concentration [38]. But this mechanism cannot explain Mg uptake in planktonic foraminifera as the culture experiments indicate that Mg/Ca ratios decrease with increasing pH [38]. Clearly, it is problematic to explain the nature of the Mg/Ca peak at the Eocene/Oligocene boundary; too little is known about Mg uptake into benthic foraminiferal tests. Because of these factors, we are cautious with paleoceanographic interpretations of the site 689 Mg/Ca record across this climate transition.

### 4.3. Evolution of Cenozoic ice volume

The Mg/Ca-based $\delta^{18}O_{sw}$ reconstructions from sites 757 and 689 provide evidence for ice growth starting by $\sim 40$ Ma. Assuming a $^{18}O$-depleted late Pleistocene ice sheet with a $\delta^{18}O$ value of $-35\text{‰}$, the $0.4\text{‰}$ increase in $\delta^{18}O_{sw}$ between $\sim 40$ and 36 Ma (Fig. 3) indicated by both of our records supports growth of Antarctic ice equal to 25% of the modern cryosphere. If we allow for an ice sheet with a $\delta^{18}O$ value of up to $-17\text{‰}$ due to likely warmer polar climates [2], the volume of ice is correspondingly higher, but no more than 50% of the modern. These results are consistent with other foraminiferal-based reconstructions that have suggested presence of ice during the middle to late Eocene [46]. Other

geochemical evidence, changes in the percent illite and chlorite to Southern Ocean sediments, indicates glacial activity on Antarctica at 38–39 Ma [47]. At the Eocene/Oligocene boundary, there is an $\sim 1\text{‰}$ increase in the $\delta^{18}O_{sw}$ [6], and our smoothed $\delta^{18}O_{sw}$ records from sites 757 and 689 agree with this reconstruction (Fig. 3, bottom panel). Assuming an $^{18}O$-depleted ice sheet with a $\delta^{18}O$ value of $-35\text{‰}$, one arrives at an ice volume equivalent to the modern cryosphere, which includes an ice sheet on Greenland. Add to that the volume of ice present prior to this event, we are lead to conclude that early Oligocene ice extent was comparable to that of the Pleistocene, which leads us to speculate that ice may have existed in the Northern Hemisphere as well.

After the Eocene/Oligocene boundary, parallel trends among the $\delta^{18}O_{sw}$ records of Lear et al. [6] from site 757 and the Southern Ocean record from site 747 [7] allow for confidence in determining the timing of large-scale ice volume changes (Fig. 3). Accordingly, there have been three times of reduced global ice volumes, during the late Oligocene ($\sim 26$ Ma), the early Miocene ($\sim 16$ Ma), and the Pliocene ($\sim 2$–4 Ma). The late Oligocene and early Miocene $\delta^{18}O_{sw}$ minima are consistent with minima in the benthic foraminiferal $\delta^{18}O$ record, but the Pliocene deglaciation event is not. The possibility of a Pliocene melt-back in Antarctic ice is particularly intriguing because of the debate that still surrounds the stability of the Antarctic ice sheet during this period of time. The foraminiferal $\delta^{18}O$ record has long been taken as evidence against Antarctic deglaciation [48]. In view of the $\delta^{18}O_{sw}$ reconstruction presented here, it appears that a fresh look at the issue of Antarctic ice sheet stability is warranted.

Relatively large offsets among the $\delta^{18}O_{sw}$ records develop after the Eocene/Oligocene boundary. Constant offsets such as during the early Miocene may incorporate the effects of interspecies differences, but temporal changes in inter-site gradients between the intermediate water sites and the composite record of Lear et al. [6] (deep water sites, Table 1) such as beginning during the middle Miocene may reflect a regional change in the $\delta^{18}O$ value of the water masses. Late Pleistocene

offsets among the three sites are difficult to explain, only the maximum $\delta^{18}O_{sw}$ values of 1‰ from site 747 agree with the values derived from the geochemistry of pore fluids [26]. The temporal resolution of the composite record of Lear et al. [6] is low, and the true amplitude of the Mg/Ca signal may have been aliased. As noted above, the most recent $\delta^{18}O_{sw}$ values from site 757 are higher than what can be expected based on modern ocean intermediate water hydrography. We speculate that Plio/Pleistocene Mg/Ca ratios at this site may be contaminated with high-Mg calcite, which appears to be a possibility at other warm, relatively shallow water depths (Little Bahama Bank, Lear et al. [19]).

## 5. Conclusion

We present two new benthic foraminiferal Mg/Ca records from intermediate water depth sites to reconstruct paleotemperatures as a means to infer changes in the $\delta^{18}O_{sw}$ related to Antarctic cryosphere development during the Cenozoic (0–52 Ma). Together with published records our results indicate that Mg-derived paleotemperatures are highly sensitive to assumptions about seawater Mg/Ca ratios. Using the oxygen isotope paleothermometer to provide a temperature constraint during presumable ice-free conditions (middle Eocene) we observe that a good match can be achieved with Mg/Ca-derived temperatures if we assume modern seawater ratios, or ratios at most 0.5 molar ratios lower than today. An increase in $\delta^{18}O_{sw}$ begins at at least $\sim$40 Ma, which supports studies that have proposed a middle Eocene, or earlier, onset of Antarctic glaciation. An increase in Mg/Ca ratios at the Eocene/Oligocene boundary apparent at Weddell Sea site 689 could be interpreted as a high latitude warming concurrent with the major phase of Antarctic ice sheet expansion. However, we caution that these results may provide an example of additional biogeochemical controls on the partitioning coefficient for Mg in benthic foraminiferal calcite. During the Neogene, agreement in trends between the $\delta^{18}O_{sw}$ and the global benthic foraminiferal $\delta^{18}O$ record exists in the timing of ice volume changes during the late Oligocene and Miocene, but not the Pliocene. During the Pliocene two of the $\delta^{18}O_{sw}$ records display a minima, which would be more consistent with those scenarios that have argued for Antarctic deglaciation. Although $\delta^{18}O_{sw}$ values become unrealistically high at site 757 during the Plio/Pleistocene, maximum Pleistocene $\delta^{18}O_{sw}$ values at site 747 are in excellent agreement with the $\delta^{18}O_{sw}$ derived from other geochemical proxies. This observation underscores the value of the new Mg/Ca-temperature calibrations of Martin et al. [10] and Lear et al. [19].

## References

[1] N.J. Shackleton, J.P. Kennett, Paleotemperature history of the Cenozoic and the initiation of Antarctic glaciation: Oxygen and carbon isotopic analyses in DSDP Sites 277, 279, and 281, Init. Rep. Deep Sea Drill. Proj. 29 (1975) 743–755.

[2] K.G. Miller, R.G. Fairbanks, G.S. Mountain, Tertiary oxygen isotope synthesis, sea level history, and continental margin erosion, Paleoceanography 2 (1987) 1–19.

[3] J.C. Zachos, M. Pagani, L. Sloan, E. Thomas, K. Billups, Trends, rhythms and aberrations in global climate 65 Ma to present, Science 292 (2001) 686–693.

[4] T.A. Mashiotta, D.W. Lea, H.J. Spero, Glacial-interglacial changes in subantarctic sea surface temperature and the $\delta^{18}O$ of seawater using foraminiferal Mg, Earth Planet. Sci. Lett. 170 (1999) 417–432.

[5] D.W. Lea, D.K. Pak, H.J. Spero, Climate impact of Late Quaternary equatorial Pacific sea surface temperatures, Science 289 (2001) 1719–1723.

[6] C.H. Lear, H. Elderfield, P.A. Wilson, Cenozoic deep-sea temperatures and global ice volumes from Mg/Ca in benthic foraminiferal calcite, Science 287 (2000) 269–272.

[7] K. Billups, D.P. Schrag, Paleotemperatures and ice-volume of the past 27 myr revisited with paired Mg/Ca and stable isotope measurements on benthic foraminifera, Paleoceanography 17 (2002) 10.1029/2000PA000567.

[8] J.G. Sclater, E. Boyle, J.M. Edmond, A quantitative analysis of some factors affecting carbonate sedimentation in the oceans, in: Deep Drilling Results in the Atlantic Ocean: Continental Margin and Paleoenvironment (1979) 235–248.

[9] S.J. Brown, H. Elderfield, Variations in Mg/Ca and Sr/Ca ratios of planktonic foraminifera caused by postdepositional dissolution: Evidence of shallow Mg-dependent dissolution, Paleoceanography 11 (1996) 543–551.

[10] P.A. Martin, D.W. Lea, Y. Rosenthal, N.J. Shackleton, M. Sarnthein, T. Papenfuss, Quaternary deep sea temperature history derived from benthic formaniferal Mg/Ca, Earth Planet, Sci. Lett. 198 (2002) 193–209.

[11] D.P. Schrag, D.J. dePaolo, F.M. Richter, Reconstructing past sea surface temperatures: Correcting for diagenesis of bulk marine carbonate, Geochim. Cosmochim. Acta 59 (1995) 2265–2278.

[12] Shipboard Scientific Party, site 757, in: J. Pierce, J. Weissel et al. (Eds.) Proc. ODP Init. Rep. 121, College Station, TX (1989) 305–358.

[13] H.S. Ostlund, H. Craig, W.S. Broecker, D. Spencer, GEOSECS Atlantic, Pacific, and Indian Ocean Expedition, 7, Shorebased Data and Graphics, National Science Foundation, Washington, DC (1987) 200 pp.

[14] J.P. Kennett, L.D. Stott, Proteus and Propo-Oceanus: Ancestral Paleogene oceans as revealed from Antarctic stable isotopic results; ODP Leg 113, in: P.F. Barker, J.P. Kennett et al. (Eds.), Proc. ODP Sci Results 113, College Station, TX (1990) pp. 865–880.

[15] W.A. Berggren, D.V. Kent, C.C. Swisher, III, M.P. Aubry, A revised Cenozoic geochronology and chronostratigraphy, in: W.A. Berggren, D.V. Kent, M.-P. Aubry, J. Hardenbol (Eds.), Geochronology, Time Scales and Stratigraphic Correlation, SEPM (Society for Sedimentary Geology), Special Publication 54 (1995) pp. 129–212.

[16] W.A. Berggren, F.J. Hilgren, C.G. Langereis, D.V. Kent, J.D. Obradovitch, I. Raffi, M.E. Raymo, N.J. Shackleton, Late Neogene chronology: New perspectives in high-resolution stratigraphy, Geol. Soc. Am. Bull. 107 (1995) 1272–1287.

[17] W. Hastings, A.D. Russell, S.R. Emerson, Foraminiferal magnesium in *Globigerinoides sacculifer* as a paleotemperature proxy, Paleoceanography 13 (1998) 161–169.

[18] P.A. Martin, D.W. Lea, A simple evaluation of cleaning procedures on fossil benthic formaniferal Mg/Ca, Geochem. Geophys. Geosyst. (in press).

[19] C.H. Lear, Y. Rosenthal, N. Slowey, Benthic formaniferal Mg/Ca-paleothermometry: A revised core-top calibration, Geochim. Cosmochim. Acta (in press).

[20] D.P. Schrag, Rapid analysis of high-precision Sr/Ca ratios in corals and other marine carbonates, Paleoceanography 14 (1999) 100–102.

[21] Y. Rosenthal, E.A. Boyle, N. Slowey, Temperature control on the incorporation of magnesium, strontium, fluorine, and cadmium into benthic foraminiferal shells from Little Bahama Bank: Prospects for thermocline paleoceanography, Geochim. Cosmochim. Acta 61 (1997) 3633–3643.

[22] N.J. Shackleton, Attainment of isotopic equilibrium between ocean water and the benthonic foraminifera genus *Uvigerina*: Isotopic changes in the ocean during the last glacial, Cent. Nat. Sci. Colloq. Int. 219 (1974) 203–209.

[23] N.J. Shackleton, N.D. Opdyke, Oxygen isotope and paleomagnetic stratigraphy for equatorial Pacific core V28-238: oxygen isotope temperatures and ice volumes on a $10^5$ year and $10^6$ year scale, Quat. Res. 3 (1973) 39–55.

[24] E. Boyle, L.D. Keigwin, Comparison of Atlantic and Pacific paleochemical records for the last 250,000 years changes in deep ocean circulation and chemical inventories, Earth Planet. Sci. Lett. 76 (1985) 135–150.

[25] D.J. Nuernberg, J. Bijma, C. Hemleben, Assessing the reliability of magnesium in foraminiferal calcite as a proxy for water mass temperature, Geochem. Cosmochem. Acta 60 (1996) 803–814.

[26] D.P. Schrag, G. Hampt, D.W. Muray, Pore fluid constraints in the temperature and oxygen isotopic composition of the glacial ocean, Science 272 (1996) 1930–1932.

[27] B.H. Wilkinson, T.J. Algeo, Sedimentary carbonate record of calcium-magnesium cycling, Am. J. Sci. 289 (1989) 1158–1194.

[28] J.I. Drever, Y.H. Li, B. Maynard, Geochemical cycles-the continental crust and the oceans, in: C.B. Gregor, R.M. Garrels, R.F.T. Mackenzie, J.B. Maynard (Eds.), Chemical Cycles in the Evolution of the Earth, Wiley Interscience, New York (1988) pp. 17–25.

[29] J.M. Gieskes, J.R. Lawrence, Alteration of volcanic matter in deep sea sediments-evidence from the chemical composition of interstitial waters from deep sea drilling cores, Geochim. Cosmochim. Acta 45 (1981) 1687–1703.

[30] H. Elderfield, A. Schultz, Mid-ocean ridge hydrothermal fluxes and the chemical composition of the ocean, Annu. Rev. Earth Planet. Sci. 24 (1996) 191–224.

[31] S.M. Stanley, L.A. Hardie, Secular oscillations in the carbonate mineralogy or reef-building and sediment producing organisms driven by tectonically forced shifts in seawater chemistry, Palaeogeogr. Palaeoclimatol. Palaeoecol. 144 (1998) 3–19.

[32] R.M. Owen, D.K. Rea, Sea floor hydrothermal activity links climate to tectonics: The Eocene $CO_2$ greenhouse, Science 227 (1985) 166–169.

[33] D.K. Rea, M. Leinen, Neogene controls on hydrothermal activity and paleoceanography of the southwest Pacific Ocean, in: M. Leinen, D.K. Re et al. (Eds.), Init. Rep.

Deep Sea Drill. Proj. 92, U.S. Government Printing Office, Washington, DC, 1986, pp. 597–617.

[34] M.J. Mottl, G. Wheat, Hydrothermal circulation through mid-ocean ridge flanks: Fluxes of heat and magnesium, Geochim. Cosmochim. Acta 58 (1994) 2225–2237.

[35] H. Zimmermann, Tertiary seawater chemistry-implications from primary fluid inclusions in marine halite, Am. J. Sci. 300 (2000) 723–767.

[36] T.K. Lowenstein, M.N. Timofeff, S.T. Brennan, L.A. Hardie, R.V. Demicco, Oscillations in Phanerozoic seawater chemistry: Evidence from fluid inclusions, Science 294 (2001) 1086–1088.

[37] M.L. Prentice, R.K. Matthews, Tertiary ice sheet dynamics: the snow gun hypothesis, J. Geophys. Res. 96 (1991) 6811–6827.

[38] D.W. Lea, T.A. Mashiotta, H.J. Spero, Controls on magnesium and strontium uptake in planktonic foraminifera determined by live culturing, Geochim. Cosmochim. Acta 63 (1999) 2369–2379.

[39] H.M. Stoll, D.P. Schrag, Coccolith Sr/Ca as a new indicator of coccolithophorid calcification and growth rate, Geochem. Geophys. Geosyst. 1 (2000) 1999GC000015.

[40] R.E.M. Rickaby, D.P. Schrag, Growth-rate dependence of Sr incorporation during calcification of *Emiliani huxleyi*, Biogeochemical Cycles, (2002) 10.1029/2001GB001408, 2002.

[41] L. Dieter-Haass, L.R. Zahn, Eocene-Oligocene transition in the Southern Ocean: History of water mass circulation and biological productivity, Geology 24 (1996) 163–166.

[42] R.B. Lorens, Sr, Cd, Mn, and Co distribution coefficients in calcite as a function of calcite precipitation rate, Geochim. Cosmochim. Acta 45 (1981) 553–561.

[43] J.W. Morse, M.L. Bender, Partition coefficients in calcite: Examination of factors influencing the validity of experimental results and their application to natural systems, Chem. Geol. 82 (1990) 265–277.

[44] S.J. Carpenter, K.C. Lohmann, Sr/Mg ratios of modern marine calcite: Empirical indicators of ocean chemistry and precipitation rate, Geochim. Cosmochim. Acta 56 (1992) 1837–1849.

[45] H.M. Stoll, D.P. Schrag, Sr/Ca variations in Cretaceous carbonates relation to productivity and sea level changes, Palaeogeogr. Palaeoclimatol. Palaeoecol. 168 (2001) 311–336.

[46] J.V. Browning, K.G. Miller, D.K. Pak, Global implications of Eocene Greenhouse and Doubthouse sequences on the New Jersey coastal plain – The Icehouse cometh, Geology 24 (1996) 639–642.

[47] J.C. Zachos, B.N. Opdyke, T.M. Quinn, E.C. Jones, A.N. Halliday, Early Cenozoic glaciation, Antarctic weathering, and seawater 87Sr/86Sr: is there a link?, Chem. Geol. 161 (1999) 165–180.

[48] J.P. Kennett, D.A. Hodell, Evidence for relative climate stability of Antarctica during the early Pliocene: A marine perspective, Geograf. Ann. 75 (1993) 205–220.